Synthesis and Characterization of Superparamagnetic Ni−Pt Nanoalloy

Madhuri Mandal,[†] Subrata Kundu,[†] Tapan K. Sau,[‡] S. M. Yusuf,[§] and Tarasankar Pal*[,†]

Department of Chemistry, Indian Institute of Technology, Kharagpur-721302, India, CAMP, Clarkson University, Potsdam, New York 13699-5814, and Solid State Physics Division, Bhabha Atomic Research Center, Mumbai, India

Received February 28, 2003. Revised Manuscript Received June 19, 2003

A room-temperature wet chemical method of synthesis for sphere- and rod-shaped magnetic "solid solution" type Ni−Pt nanoparticles in cetyltrimethylammonium bromide (CTAB) micelle is reported. The particles have been found to be moderately monodispersed without adopting any further size-selection procedure. The composition of the alloy becomes tunable through adjustment of the ratio of the reactants. The temperature-dependent magnetic property, size distribution, and percentage composition of the alloyed structures are characterized by SQUID magnetometer, transmission electron microscopy (TEM), scanning electron microscopy (SEM), and electron dispersive X-ray (EDX) analyses. The preferential evolution of nanorods over spherical particles in higher surfactant concentrations and the coalescence of the magnetic particles have been examined.

Introduction

Nanostructures with controlled size and shape are important from both fundamental and technological viewpoints.[1] There has been an unabated tendency for a long time to prepare nanoparticles of various sizes and shapes.[1a,b] In fact, it is well-known that the size and shape are two primary variables determining physical (such as magnetic, optical, etc.) as well as chemical (reactivity, catalysis, etc.) properties of nanoparticles.[1c,d] Basic and applied aspects of magnetic systems with nanoscale dimensions have been known for a long time.[2] Nanomagnets appear to be versatile for a wide range of applications in enlarged data storage, memory elements, and sensors.[2] Geometry of a nanomagnet has great impact on its magnetic properties resulting from the interplay among different types of magnetic energies. Elongated magnetic systems are of interest for binary data storage applications because they have two stable magnetization states.[2] The ability to prepare air-stable ferromagnetic noble bimetallic particles is therefore a challenge.

Preparation of Ni nanoparticles by the reduction of aqueous nickel salt alone by common reducing agents is very difficult[3] even in the presence of strong alkali. Y.-P. Sun and co-workers[4] synthesized ∼5-nm-size Ni particles via a combination of rapid expansion of supercritical fluid solutions and chemical reduction, whereas Reetz and Helbig[5] used an electrochemical method. Duteil et al.[6] synthesized similar-sized ligand-stabilized nickel nanoparticles in a nonaqueous medium. Relatively large size (∼60 nm) spherical Ni particles have been prepared by Zheng et al.[7] in an ethanol−water solvent system. Recently, Sun et al.[8] and Nunomora et al.[9] prepared spherical bimetallic magnetic nanoparticles of Fe−Pt and Ni−Pd, respectively, via a solution-phase alcohol reduction method. Very recently, Ni nanowires of 5−25 μm length have been prepared by electrochemical growth in alumina filter templates.[10] We report here a very simple solution-phase wet chemical reduction method of preparation to obtain moderately monodispersed rod-shaped superparamagnetic Ni−Pt particles using an aqueous mono-surfactant system. To our knowledge, there has been no method simpler than this available for the preparation of such rod-shaped nanomagnets. This method of preparation is very simple, fast, and reproducible, and also suitable for large-scale synthesis. In addition, Ni−Pt particles are of interest for their catalytic properties. These nanomagnets are of small length (∼20 nm), which might render them a promising candidate for data storage applications. Furthermore, because of their magnetic

* To whom correspondence should be addressed. E-mail: tpal@chem.iitkgp.ernet.in.
[†] Indian Institute of Technology.
[‡] CAMP, Clarkson University.
[§] Bhabha Atomic Research Center.

(1) (a) Xia, Y.; Gates, B.; Yin, Y.; Lu, Y. *Adv. Mater.* **2000**, *12*, 693. (b) Adair, J. H.; Suvaci, E. *Curr. Opin. Colloid Interface Sci.* **2000**, *5*, 160. (c) Legrand, J.; Petit, C.; Pileni, M. P. *J. Phys. Chem. B* **2001**, *105*, 5643. (d) Sau, T. K.; Pal, A.; Pal, T. *J. Phys. Chem. B* **2001**, *105*, 9266.
(2) Kirk, K. J. *Contemp. Phys.* **2000**, *41*, 61.
(3) Glavee, G. N.; Klabunde, K. J.; Sorensen, C. M.; Hadjipanayis, G. C. *Inorg. Chem.* **1993**, *32*, 474.
(4) Sun, Y.-P.; Rollins, H. W.; Guduru, R. *Chem. Mater.* **1999**, *11*, 7.
(5) Reetz, M. T.; Helbig, W. *J. Am. Chem. Soc.* **1994**, *116*, 7401.
(6) Duteil, A.; Schmid, G.; Meyer-Zaika, W. *J. Chem. Soc. Chem. Commun.* **1995**, 31.
(7) Zheng, H.; Liang, J.; Zeng, J.; Qian, Y. *Mater. Res. Bull.* **2001**, *36*, 947.
(8) Sun, S.; Murray, C. B.; Weller, D.; Folks, L.; Moser, A. *Science* **2000**, *287*, 1989.
(9) Nunomora, N.; Hori, H.; Teranishi, T.; Miyake, M.; Yamada, S. *Phys. Lett. A* **1998**, *249*, 524.
(10) Tanase, M.; Bauer, L. A.; Hultgren, A.; Silevitch, D. M.; Sun, L.; Reich, D. H.; Searson, P. C.; Meyer, G. J. *Nano Lett.* **2001**, *1*, 155.

10.1021/cm030246d CCC: $25.00
Published on Web 08/12/2003

field of attraction, nanorods can be assembled into a number of arrays with special configurations that might give rise to many novel properties. Magnetic materials of Fe, Co, and Ni are quite unstable with respect to both coagulation and reactivity. Therefore, preparations of magnetic nanoparticles have been carried out in the presence of various stabilizing agents.[6,11] One important characteristic of organic macromolecules is their predisposition to form liquid crystalline phases when they possess a rodlike shape.[12] We have used a well-known surfactant, cetyltrimethylammonium bromide (CTAB) as stabilizing/capping agent[13] which simultaneously serves the purpose of a template. At higher concentration, it acts as a template in such a fashion that the number of rod-shaped particles becomes more prevalent.[14] The advent of new methods for preparing highly soluble and processable colloidal metallic, semiconductor, and magnetic nanocrystals with very tight control over size and shape creates significant opportunities in the study of inorganic liquid crystals.

Experimental Section

Reagents and Instruments. $NiSO_4 \cdot 7H_2O$ (BDH, India), H_2PtCl_6 (Johnson Matthey), and CTAB (Loba Chemie, India) were used. All the other reagents used were of AR grade. Solutions were prepared in double-distilled water and diluted to different concentrations as necessary. TEM and SEM studies were performed using Hitachi S-4300 and G-1 JEOL JFM 5800 (Japan), respectively, evaporating the sample on carbon-coated copper grid.

Procedure. Ni−Pt alloyed magnetic nanoparticles were prepared by the following method. The reaction was performed in a medium of CTAB of various concentrations 0.25 M, 0.1 M, 10^{-3} M, and 10^{-4} M (sets A, B, C, and D respectively) under N_2-atmosphere in airtight condition. At first, Ni-salt 1.4×10^{-2} M and H_2PtCl_6 4.8×10^{-4} M were taken in CTAB micellar medium. Finally, the ratio of Ni to Pt of 96:4 (by atomic) was attained. The solution was degassed by N_2 for 15 min under stirring condition, then 30 μL of hydrazine monohydrate ($N_2H_4 \cdot H_2O$), and in next step 200 μL of KOH solution (9.0 M), were injected into the reaction mixture under stirring condition. The final concentration of KOH in the solution became 0.35 M. The stirring was continued for another 15 min. Again at low temperature (~5 °C), keeping all other conditions fixed, we observed evolution of more rod particles (set E). The same reaction was performed varying the proportion of Ni and Pt in the same environment at room temperature (set F).

Results and Discussion

Reduction of Ni salt in a wet chemical method using a common reducing agent is very difficult. In the reduction process, the role of noble metal nuclei is now well-known.[15] They efficiently reduce the metal ions of Ni, Co, Fe, and Pb, etc. which otherwise do not easily yield metal cluster. Evolution of Ni−Pt alloyed nanomagnets from the corresponding salt solutions is reported here. Cationic micelle CTAB helps the stabilization of alloyed nanoparticles. Noble metal Pt(0) atom is generated first in-situ (i.e., in the reaction medium) from the H_2PtCl_6 in the presence of the well-known reducing agent $N_2H_4 \cdot H_2O$, as the standard redox potential of $PtCl_6^{2-}/Pt$ and N_2/N_2H_4 are 0.705 and 0.23 V, respectively. A small cluster can transfer an electron to many inorganic and organic molecules[16] and description of such a process could be given in terms of the standard redox potential $E°$ (M^+/M_n) of the metal as a function of the agglomeration number, n. If in a solution both a particulate of a metal and its ions are present together, then the typical metal electrode equilibrium can be expressed as follows.

$$M_{n-1} + M^{x+} + xe^- = M_n$$

During the growth of such small scale particles their redox potential varies continuously.[17] The redox potential of the particle for a particular metal depends on the value of the agglomeration number n and the nature of associated ligand. For example the redox potential is as negative as −2.7, −1.8, and −1.5 V (vs NHE) for $n =$ 1 for Cu, Ag, and Au, respectively.[17a,18] The potential becomes more and more positive as the particles grow and reach their respective value of bulk state. Here, as soon as Pt atom is formed its $E°$ value reaches to more negative than that of the $Ni(OH)_2/Ni$ system ($E° = -0.72$ V), and as a result Ni^{2+} ions get adsorbed on Pt(0) and simultaneously reduced to Ni(0) and thus autocatalytically generate the alloyed nanomagnets through competitive coreduction of both the metal ions (Pt^{4+} and Ni^{2+}). Shape and size of the particles are tuned by varying the concentrations of micelles and salts. The same reaction was performed under identical conditions but in the absence of Pt salt. In that case no reduction of Ni salt took place. Hence, it is clear from this phenomenon that at the beginning the Pt ion is reduced to an atom of Pt(0), which then catalyzes the reduction of Ni(II) to Ni(0) as well as Pt(IV) to Pt(0) by hydrazine, and consequently generates solid-solution type Ni−Pt magnetic nanoparticles. The TEM and EDX study did not reveal the indication of any "core−shell" structure just like the seeding growth of the particles.[19] Instead alloying took place, which might be due to simultaneous reduction of both the metal ions, and stirring might have a bearing on the synthesis. The reported method could be a model for the formation of different nanoalloys. Moreover precious metals such as Pt could be saved by optimizing the synthetic condition so that a very small amount of it is utilized for the alloy formation by this method.[20] Reducing agents such as ascorbic acid, HCHO, CO, and even UV light with variable flux could not produce bimetallic nanoparticles under the said experimental condition.

The composition of selected nanoparticles was determined by energy-dispersive X-ray (EDX) analysis. In

(11) Ely, T. O.; Amiens, C.; Chaudret, B. *Chem. Mater.* **1999**, *11*, 526.
(12) Alivisatos, A. P. *Science* **1996**, *271*, 933.
(13) Bonnemann, H.; Binkmann, R.; Neileler, P. *Appl. Organometallic Chem.* **1994**, *8*, 361.
(14) Jana, N. R.; Gearheart, L.; Murphy, C. J. *Adv. Mater.* **2001**, *13*, 1389.
(15) (a) Treguer, M.; de Cointet, C.; Remita, H.; Khatouri, J.; Mostafavi, M.; Amblard, J.; Belloni, J.; de Keyzer, R. *J. Phys. Chem. B* **1998**, *102*, 4310. (b) Marignier, J. L.; Belloni, J.; Delcourt, M. O.; Chevalier, J. P. *Nature* **1985**, *317*, 344.
(16) Henglein, A. *Israel J. Chem.* **1993**, *33*, 77.
(17) (a) Henglein, A. *Chem. Rev.* **1989**, *9*, 1861. (b) Mostafavi, M.; Marignier, J. L.; Amblard, J.; Belloni, J. *Radiat. Phys. Chem.* **1989**, *34*, 605. (c) Henglein, A. *J. Phys. Chem.* **1993**, *97*, 5457.
(18) (a) Belloni, J. *Curr. Opin. Colloid Interface Sci.* **1996**, *1*, 184. (b) Mosseri, S.; Henglein, A.; Janata, E. *J. Phys. Chem.* **1989**, *93*, 6791.
(19) Mallik, K.; Mandal, M.; Pradhan, N.; Pal, T. *Nano Lett.* **2001**, *1*, 319.
(20) Schmid, G.; Lehnert, A.; Malm, J. O.; Bovin, J. O. *Angew. Chem. Int. Ed.* **1991**, *30*, 874.

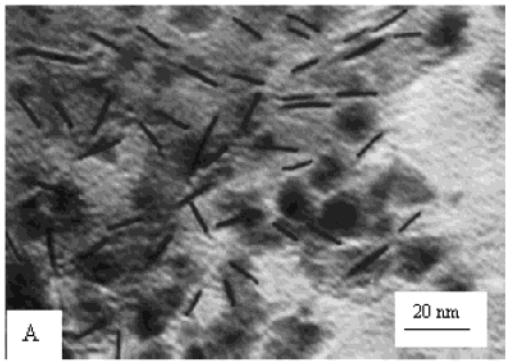
A
20 nm

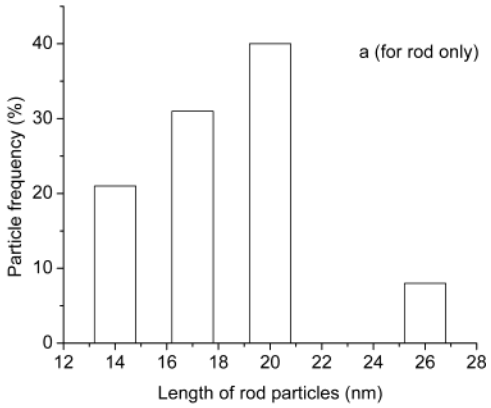
a (for rod only)
Particle frequency (%)
0
10
20
30
40
12
14
16
18
20
22
24
26
28
Length of rod particles (nm)

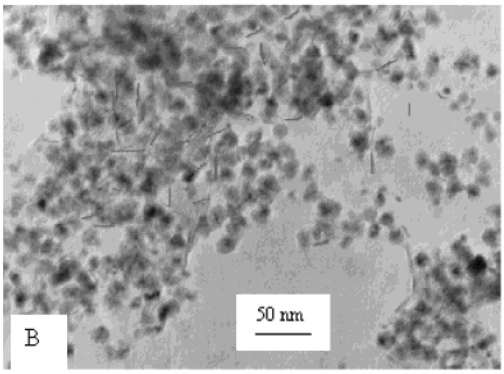
B
50 nm

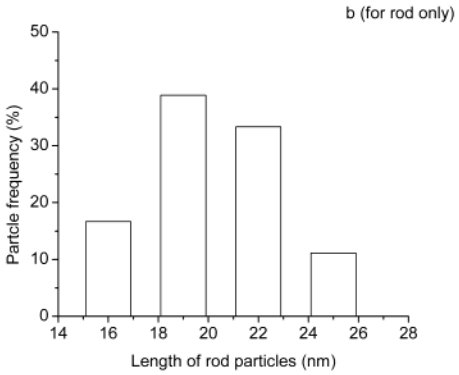
b (for rod only)
Partcle frequency (%)
0
10
20
30
40
50
14
16
18
20
22
24
26
28
Length of rod particles (nm)

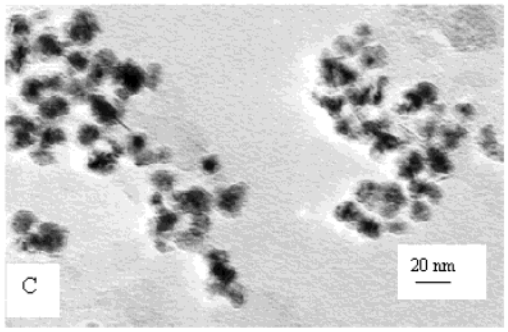
C
20 nm

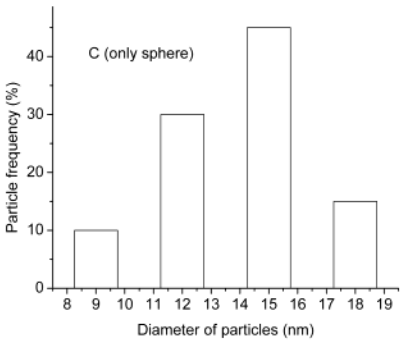
C (only sphere)
Particle frequency (%)
0
10
20
30
40
8
9
10
11
12
13
14
15
16
17
18
19
Diameter of particles (nm)

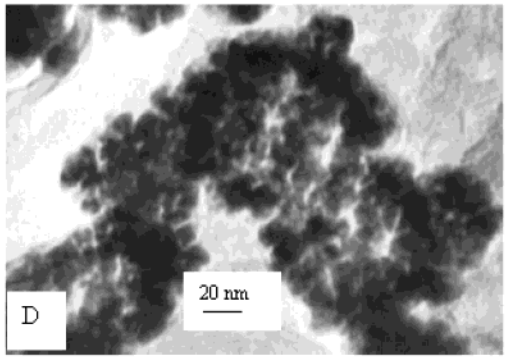
D
20 nm

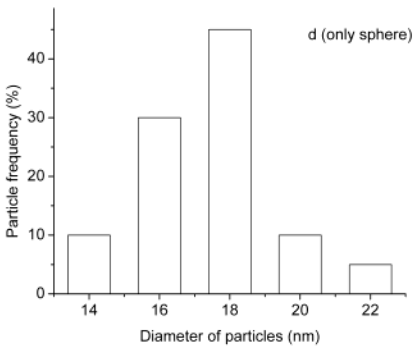
d (only sphere)
Particle frequency (%)
0
10
20
30
40
14
16
18
20
22
Diameter of particles (nm)

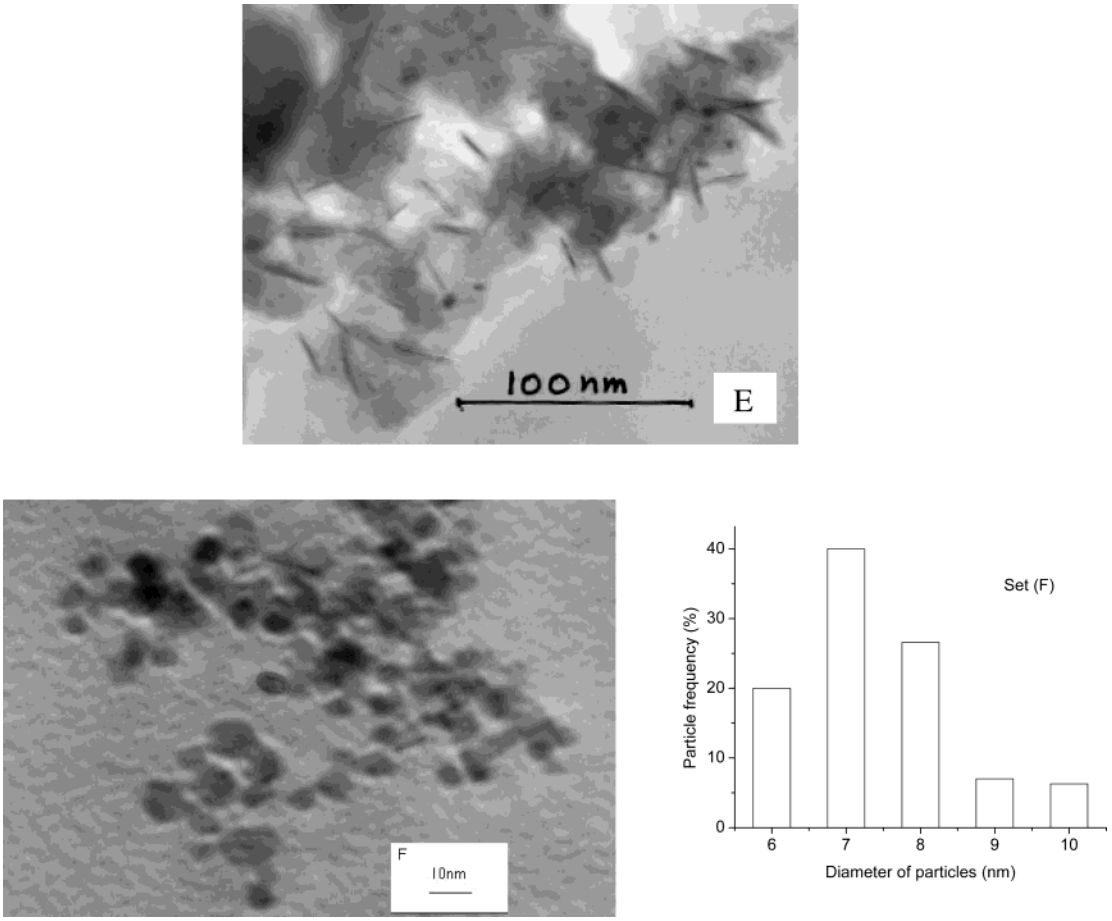

Figure 1. Transmission electron micrograph (TEM) of Ni−Pt bimetallic nanoparticles. Condition: $[NiSO_4] = 1.4 \times 10^{-2}$ M, $[H_2PtCl_6] = 4.8 \times 10^{-4}$ M, [KOH] = 0.36 M for all the sets. [CTAB] = 0.25 M, 0.1 M, 10^{-3} M, 10^{-4} M, and 0.1 M for (A), (B), (C), (D), and (E), respectively. Samples (A), (B), (C), and (D) were synthesized at room temperature (25 °C), and sample (E) was synthesized at 5 °C. For set (F) $[NiSO_4] = 4.3 \times 10^{-3}$ M, $[H_2PtCl_6] = 2.44 \times 10^{-3}$ M, [CTAB] = 0.1 M, and [KOH] = 0.36 M, and temperature = 25 °C.

Table 1. EDX Data for Three Different Spherical Particles from Set B

element	atomic %	atomic %	atomic %
Ni	96.06	97.11	96.12
Pt	3.94	2.89	3.88

Table 2. EDX Data for Three Different Rod-Shaped Particles from Set B

element	atomic %	atomic %	atomic %
Ni	96.89	95.99	97.24
Pt	3.11	4.01	2.76

this analysis the incident electron beam was located on a single particle of interest and the X-ray fluorescence from that particle was measured. It was compared with the background spectra measured from a point where no particle was observed. The EDX analyses from different spherical and-rod shaped particles authenticate that all the particles are homogeneous and hence alloyed together in Ni−Pt nanoparticles. Results of EDX data analyses of set (B) for different spheres and rods are given in Tables 1 and 2. Variation of a wide range of concentrations of CTAB surfactant from lower to higher (10^{-4} to 0.25 M) interestingly showed the trend of formation of a larger number of rod-shaped particles (Figure 1). TEM images showed that a large proportion of nanorods of length ∼20 nm (aspect ratio ∼7) along with spherical particles (∼10 nm) are evolved at a higher concentration of CTAB (0.25 M), and the proportion of spheres of bigger size increases with decrease of CTAB concentration. Considering only spherical particles the standard deviations in size for all the sets A, B, C, and D in Figure 1 are 9 ± 1, 12 ± 1.5, 15 ± 2, and 18 ± 3, respectively. Taking the length of the nanorods into consideration, the standard deviations in length are 19 ± 3 nm and 20 ± 2.75 nm for the sets A and B, respectively. A decrease in the size of nanoparticles means an increase in reactivity; hence, small particles are very much reactive, and because of their inherent magnetic properties they aggregate. Separation of rod-shaped particles from the mixture containing rods and spheres is very difficult because of their inherent magnetic property. Moreover, the presence of a higher concentration of surfactant makes the TEM measurement difficult. So most of the measurements were done for the sample prepared in 0.1 M CTAB. Again, the investigation was performed with a lowered temperature of the reaction medium. During synthesis at 5 °C the evolution of a higher proportion of rod-shaped particles was observed (Figure 1E) in comparison to that observed for the synthesis at room temperature. Changing the proportion of Ni to Pt (Ni/Pt = 64:36) the size distribution (Figure 1F) and magnetic properties were also investigated. By increasing the Pt proportion we got smaller size particles ($\sim 7 \pm 0.5$), which may be due to a higher number of nuclei formed which leads to

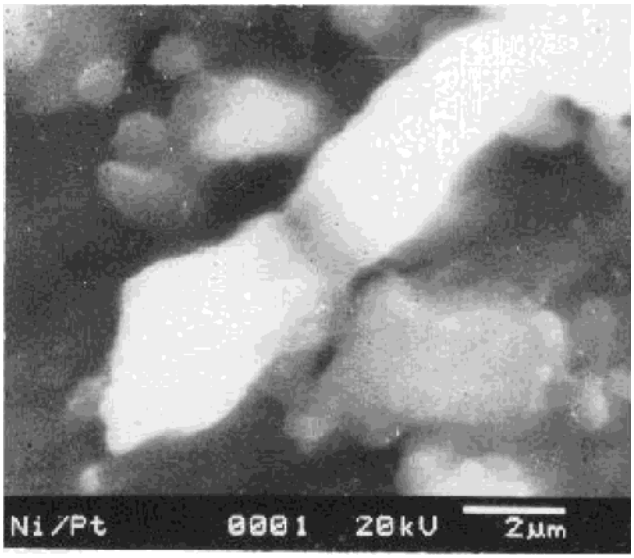

Figure 2. Scanning electron micrograph (SEM) of Ni−Pt nanomagnets (sample B). Condition: $[NiSO_4] = 1.4 \times 10^{-2}$ M, [KOH] = 0.36 M, [CTAB] = 0.1 M, and $[H_2PtCl_6] = 4.8 \times 10^{-4}$ M.

smaller particles. Water suspension of the particles under an ordinary microscope helped in visualizing their movements (for aggregation) even on a glass slide. Impact of the water molecules on the magnetic particles was that they could not resist their tendency of aggregation.

SEM study (Figure 2) showed relatively larger particles than those observed from the TEM study. This is because higher temperature (∼1000 °C) during carbon coating led to the fusion of particles in a linear fashion. This sort of linear aggregation is due to the uneven distribution of surface energy of the nonspherical particles.[21] Even after fusion during SEM measurements EDS analysis also revealed the homogeneity of Ni and Pt distribution in the particles and these fused nanomagnets consist of 96.5% (atomic) Ni and 3.5% (atomic) Pt, which is exactly equal to the Ni/Pt (atomic) taken from standard solutions for the preparation of the sample solution. Hence, complete reduction of Ni and Pt from their corresponding ionic state to metallic state took place. The precious metal Pt was taken in very low percentage, optimizing the synthetic condition to save precious metals such as Pt. The resultant alloyed metal cluster has been exploited as selective catalyst also (discussed elsewhere).

The binding energies from the X-ray photoelectron spectroscopy (XPS) (Figure 3) study for Ni−Pt nanoalloy were calculated and compared with the literature values for Ni and Pt.[22] According to literature in XPS study most intense peak for Ni arises at 855 eV attributed to $2p_3$ of Ni and 2nd intense peak arises at 873 eV attributed to $2p_1$ of Ni. Similarly for Pt most intense peak arises at 73 eV attributed to $4f_1$ of Pt. But in the Figure 3 we noticed most intense peak for Ni arises at 865 eV (peak b) and that for Pt arises at 80 eV (peak

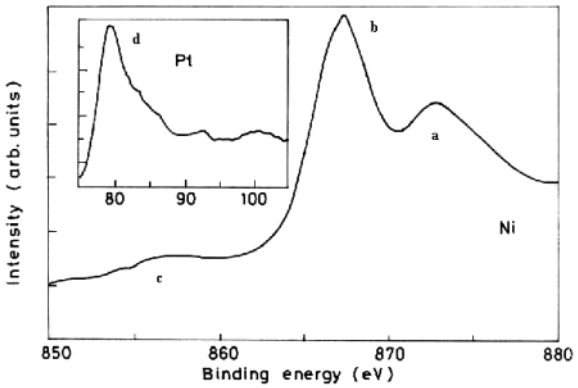

Figure 3. X-ray photoelectron spectroscopy (XPS) of Ni−Pt nanomagnets (sample B). Condition: $[NiSO_4] = 1.4 \times 10^{-2}$ M, [KOH] = 0.36 M, [CTAB] = 0.1 M, and $[H_2PtCl_6] = 4.8 \times 10^{-4}$ M.

d). Here we observed for both the cases shifting in binding energy takes place to higher energy, which is due to alloying of Ni and Pt. The peak 'a' attributed to $2p_1$ of Ni. XPS analysis is done on the surface of the particles. Here we obtained the peaks for both the metals Pt and Ni, which again authenticate the alloying of particles not the core shell type. Peak 'c' attributed to $2p_3$ of pure 'Ni' it arises because very small quantity (negligible) of Ni may not be involved in alloy formation.

The temperature-dependent magnetization of Ni−Pt nanoparticles was studied by superconducting quantum interference device (SQUID) between 5 and 300 K using zero-field-cooling (ZFC) and field-cooling (FC) procedures in an applied field of 500 Oe. This study indicates that particles at room temperature are not ferromagnetic, but rather show superparamagnetic behavior. Here it is observed that the "blocking temperature" (T_b) for the samples increases (from 65 to 150 K) with decrease of CTAB concentrations (0.25 to 10^{-4} M). It is well-known that T_b of different nanoparticles vary with the variation of particle size and shape. Two representative ZFC−FC curves for two different samples keeping the Ni/Pt proportion fixed but varying the CTAB concentrations are shown in Figure 4. Here the variation in blocking temperature is due to size and shape effect of the particles. As the CTAB concentration decreases the particle size increases, hence blocking temperature also increases. Again T_b (65 K) for the alloy having maximum rod-shaped particles was compared with that of pure Ni(0) of comparable size.[23] This difference in T_b is due to the alloying of the nanorods.[24] In this case change in blocking temperature of the alloyed particles is due to change in magnetic anisotropy from pure to alloy state.

Magnetic properties of the Ni−Pt nanoalloy were studied by varying the proportion of Ni to Pt. The magnetic studies show a hysteresis loop at 10 K for particles of different compositions of Ni and Pt, e.g., Ni/Pt 96:4 and 64:36 (Figure 5). For the former type, saturation magnetization (M_S), remanent magnetization (M_r), coercivity (H_c), and squareness ($Sr = M_r/M_S$) are 40 emu g^{-1}, 12 emu g^{-1}, 3 kOe, and 0.3, respectively,

(21) Harfenist, S. A.; Wang, Z. L.; Alverez, M. M.; Vezmar, L.; Whetten, R. L. *J. Phys. Chem.* **1996**, *100*, 13904.
(22) Briggs, D.; Seah, M. P., Eds. *Practical Surface Analysis: by Auger and X-ray Photoelectron Spectroscopy*; John Wiley & Sons: New York, 1983; appendix.
(23) Cordente, N.; Respaud, M.; Senocq, F.; Casanove, M. J.; Amiens, C.; Chaudret, B. *Nano Lett.* **2001**, *1*, 565.
(24) Pileni, M. P. *Phys. Rev. B* **2000**, *62*, 3910.

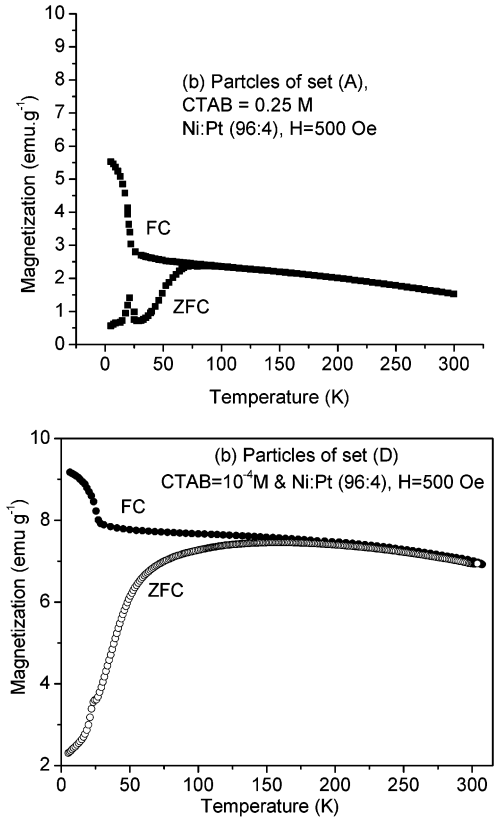

Figure 4. FC and ZFC curves for rod-shaped and spherical Ni−Pt magnetic particles of sets A and B. Condition: for both the sets $[NiSO_4] = 1.4 \times 10^{-2}$ M, [KOH] = 0.36 M, $[H_2PtCl_6] = 4.8 \times 10^{-4}$ M; but [CTAB] = 0.25 M for (a) and [CTAB] = 10^{-4} M for (b).

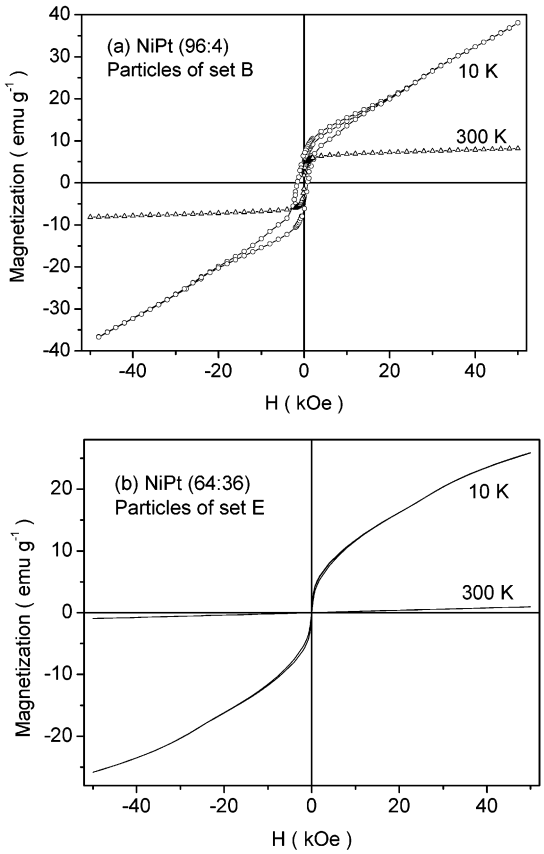

Figure 5. Hysteresis loop at 10 K for (a) Ni/Pt 96:4 (by atomic) and (b) Ni/Pt 64:36 (by atomic). Condition: [KOH] = 0.36 M, [CTAB] = 0.1 M for both the sets and for (a) $[NiSO_4] = 1.4 \times 10^{-2}$ M and $[H_2PtCl_6] = 4.8 \times 10^{-4}$ M; for (b) $[NiSO_4] = 4.3 \times 10^{-3}$ M and $[H_2PtCl_6] = 2.44 \times 10^{-3}$ M.

and for the latter type are 28 emu g^{-1}, 5 emu g^{-1}, 1 kOe, and 0.178, respectively. The higher the proportion of Ni, the higher is the saturation magnetization, higher remanence, etc., at low temperature. This also causes a larger hysteresis loop. It is evident that anisotropy is also playing an important role here. The coercivity of these ferromagnetic assemblies is tunable by controlling the Ni/Pt ratio. Ni-rich nanocrystal assemblies have the largest coercivity consistent with earlier reports.[25] Both the samples show superparamagnetic behavior at room temperature. For a superparamagnet, hysteresis is observed below blocking temperature. Above the blocking temperature there is superparamagnetic relaxation. Therefore, we do not observe any hysteresis at higher temperature, say at room temperature.

Conclusion

This kind of reaction strategy can be adapted as a general method to synthesize various types of nanoalloys with controlled composition in a selective fashion. In particular, because these magnetic alloys consist of nanorods of length ∼20 nm and aspect ratio ∼7, it is possible to have them in multidimensional arrays for magnetoelectronic nanodevice application that can fulfill the next generation requirement.

Acknowledgment. We are thankful to the Council of Scientific and Industrial Research (CSIR), New Delhi, and Department of Science and Technology (DST), New Delhi, for financial support.

CM030246D

(25) Hong, M. H.; Hono, K.; Watanabe, M. *J. Appl. Phys.* **1998**, *84*, 4403.